Nanoparticles

DOI: 10.1002/ange.200901048

Time-Resolved In Situ Synchrotron X-ray Study and Large-Scale Production of Magnetite Nanoparticles in Supercritical Water**

*Martin Bremholm, Marcella Felicissimo, and Bo B. Iversen**

Nanomaterials are of key importance owing to their dimension-dependent properties that provide novel technological applications. The magnetic properties of metal nanoparticles have been intensively explored due to their impact on the development of ultra-high-density storage media,[1] biomedical applications,[2] magnetically guided drug delivery,[3] and magnetic field cancer therapy.[4,5] Iron oxide magnetic nanoparticles are of particular interest since they are biocompatible and have low toxicity.[6]

Magnetic nanoparticles can be synthesized by several methods,[7–10] and control of particle size and particle-size distribution has been achieved. However, challenges associated with large-scale production, such as the use of organic solvents, phase purity of the nanoparticles, and long reaction times, remain.[11] In situ studies on the synthesis of nanoparticles performed in near-critical (nc) and supercritical (sc) water provide an exceptional opportunity to understand and optimize the production of nanoparticles in an environmentally friendly medium with high production rates. The most attractive feature of nc-H_2O and sc-H_2O synthesis is the possibility to tune the particle size and morphology by simply varying the pressure, temperature, and residence time. The thermal decomposition of metal precursors in a supercritical medium leads to high nucleation rates, which lead to the formation of small primary clusters.[12] We focus on the use of analytical tools capable of following nanoparticle formation and growth in real time. In situ diffraction studies are particularly suitable to achieve this goal,[13–15] but in situ studies under supercritical fluid conditions remain rare. We recently reported the first in situ study in sc-CO_2 ($P_c = 74$ bar, $T_c = 31\,^\circ C$) on the formation of TiO_2 by using simultaneous small- and wide-angle X-ray scattering (SAXS/WAXS).[16] Time-resolved SAXS/WAXS are complementary methods that enable determination of particle size, size distribution, morphology, and crystallinity. These studies also offer detailed information on the kinetics and mechanisms of nanoparticle formation.

Herein we present a time-resolved in situ study of the formation and growth of pure phase magnetite nanoparticles at much higher pressures and temperatures in nc- and sc-H_2O ($P_c = 221$ bar, $T_c = 374\,^\circ C$) using simultaneous SAXS/WAXS. To follow the formation of the product, we used a specially designed reactor and a new experimental methodology. Pulsed injections of the precursor into a reactor kept at set temperatures, as illustrated in Figure 1, were performed using a pulsed pump and a proportional relief valve that adjusts the pressure to 300 bar. High-energy X-rays are required to penetrate the steel capillary reactor capable of withstanding sc-water pressures and temperatures. The novel pulsed injection reactor avoids the severe problem of particle deposition on the reactor walls that typically makes in situ studies of continuous-flow reactions very difficult.

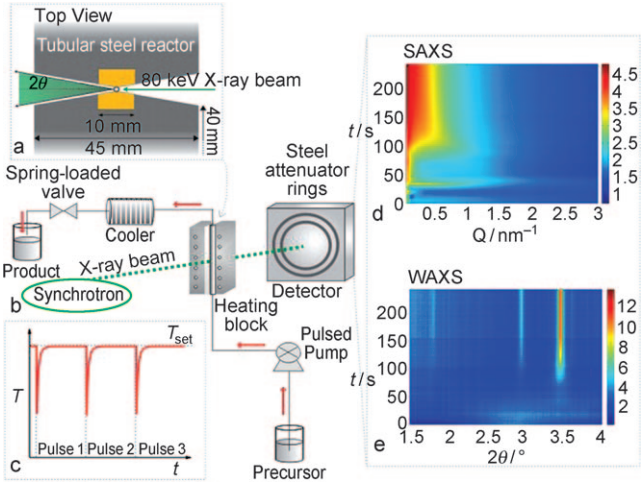

Figure 1. SAXS and WAXS in situ studies: a) Top view of the steel capillary of 2 mm inner diameter in an aluminum heating block. b) Setup applied to obtain single-phase magnetite nanoparticles in nc- and sc-water. c) Schematic temperature profile of pulsed injections. 2D color plots (relative intensities indicated by the color scale) of the data obtained by d) SAXS and e) WAXS for the experiment performed at 309 °C and 300 bar.

The SAXS and WAXS data during the first 250 s after injection of the nanoparticles at 309 °C show nucleation of magnetite after 80 s (Figure 1 d, e). The SAXS data furthermore shows the formation of an intermediate amorphous phase after 40 s. It has been observed that after nucleation of the magnetite, the nanoparticles grow continuously. The same

[*] Dr. M. Bremholm, Dr. M. Felicissimo, Prof. Dr. B. B. Iversen
Centre for Energy Materials, Department of Chemistry and iNANO
University of Aarhus
Langelandsgade 140, 8000 Aarhus C (Denmark)
Fax: (+86) 8619-6199
E-mail: bo@chem.au.dk

[**] The use of the Advanced Photon Source was supported by the US Department of Energy, Office of Science, Office of Basic Energy Sciences, under contract no. DE-AC02-06CH11357. We thank DANSCATT and SCF Technologies for funding. Jan Skov Pedersen is thanked for providing SAXS fitting software and for fruitful discussions, and Jon Almer and Mogens Christensen for help during the measurements.

Supporting information for this article is available on the WWW under http://dx.doi.org/10.1002/anie.200901048.

process was repeated at higher temperatures, such as 337, 367, and 395 °C.

To extract information regarding particle sizes, size distributions, and morphologies, the SAXS data was modeled using a sphere model and a Schulz-size distribution. By sequential least-squares refinement of the SAXS data the evolution of the numerical size distribution was determined. The unit cell dimensions, the crystallite size, and the overall scale factor were obtained by Rietveld refinement of the diffraction data.

Diffraction data provides the 'volume-averaged' crystallite sizes, which are calculated by the Scherrer equation. Sizes are weighted by $D_{PXRD} = \sqrt{\langle D^8\rangle/\langle D^6\rangle}$, where D_{PXRD} is the weighted crystallite diameter.[17] To compare sizes obtained from SAXS and WAXS directly, the number-weighted SAXS particle sizes are weighted in the same way as the Scherrer estimate. For details on SAXS modeling and refinement of the diffraction data, see the Supporting Information. Experiments were performed at four different temperatures and the sizes of the particles were determined separately by SAXS and WAXS (Figure 2a, b). The size distributions obtained from SAXS are shown in Figure 3. The plots show a relatively

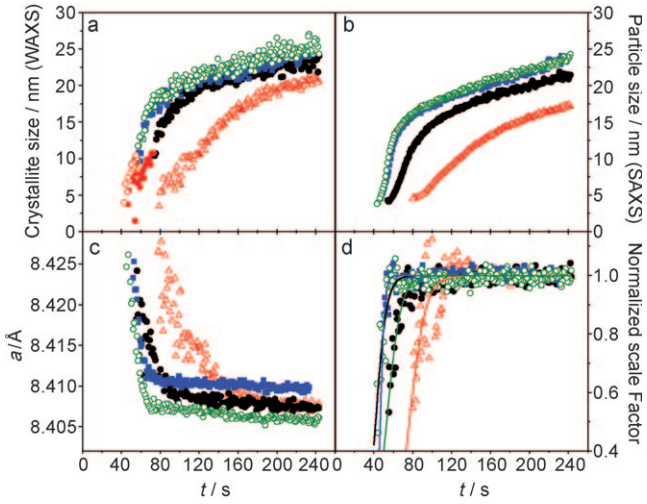

Figure 2. Magnetite nanoparticles formed in nc- and sc-H_2O. Evolution of crystallite and particle sizes determined by a) WAXS and b) SAXS. c) Unit cell dimensions (*a*) for magnetite nanoparticles and d) normalized scale factor for the synthesis of nanoparticles performed at 309 °C (△), 337 °C (●), 367 °C (■), and 395 °C (○).

slow initial stage of particle growth, followed by a sudden increase in the growth rate until the nanoparticles reach a size between 15 to 20 nm. After this stage, a slower rate in the growth of the nanoparticles is observed. Excellent agreement is observed between the SAXS and WAXS size estimates. The Rietveld refinement scale factor (Figure 2d) is a measure of the amount of crystalline material. Initially, the formation rate of the nanoparticles is high, but only a few seconds after the onset of crystallization the rate abruptly goes to zero, indicating that the precursor has been entirely consumed, rendering fully crystalline magnetite particles.

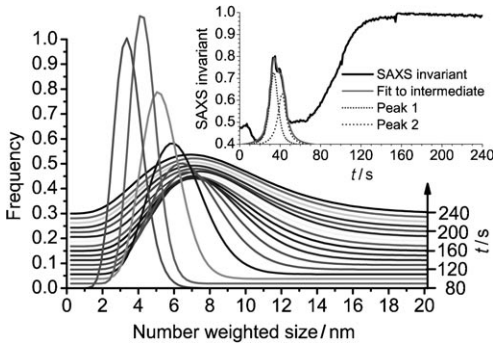

Figure 3. Size distribution as a function of time for magnetite formed at 309 °C and 300 bar. For clarity, size distributions are shown in steps of 10 seconds. The inset shows the SAXS invariant and a fit to the intermediate.

Figure 3 shows the size distribution as a function of time for magnetite nanoparticles formed at 309 °C and 300 bar. Similar plots at higher temperatures can be found in the Supporting Information. During nucleation, the size of the particle increases only slowly and the size distribution is narrow throughout the nucleation period. Therefore, fully crystalline nanoparticles with an average size of less than 10 nm and a narrow size distribution can be produced by this method if the residence time is chosen correctly. Gradually, as the particles grow there is a simultaneous broadening of the particle-size distribution, which indicates that after the initial nucleation the particles grow mainly by a coarsening mechanism.

The time-resolved in situ SAXS data indicates the formation of amorphous nanoclusters prior to crystallization (Figure 1d and Figure 3). The amorphous clusters dissolve or decompose completely, before the formation of magnetite nanocrystals. To study the amount of amorphous materials that are formed, we calculated the SAXS invariant $\int_0^\infty I(q)q^2\mathrm{d}q$, which is proportional to the volume of scattering material. At the lowest temperature, 309 °C, the invariant clearly shows two peaks separated by 6 s, which indicate that the cluster formation occurs as a two-step process (Figure 3, inset). Applying the SAXS model used for magnetite, the intermediate clusters are found to be monodisperse with a diameter of 3 nm. The particle size does not increase with time. SAXS data do not provide structural information, but it appears that the formation of the amorphous species is associated with the decomposition of the citrate, which also occurs before the nucleation of magnetite starts. One of the great advantages of the present synthesis is the use of ferrous ammonium citrate as the precursor, which results in the formation of single-phase Fe_3O_4 particles.[18,19] Iron(III) partially reduces to iron(II) owing to the formation of carbon monoxide during the thermal decomposition of the citrate. A homogeneous reaction atmosphere is provided as carbon monoxide is miscible with supercritical water, and this allows the iron oxide particles to form as single phase Fe_3O_4.[18,19] A likely explanation is that during initial heating, clusters of amorphous iron(III) hydroxide forms as an intermediate, but the reduction process induces dissolution

and recrystallization of magnetite.[20] The role of citrate and electrostatic effects merit further study.[21]

An interesting trend is that the increase in particle size is coupled to a decrease in unit cell length. This can be clearly observed in Figure 2c, which shows the unit cell dimensions for the time-resolved in situ X-ray measurements. Magnetite is the only mixed-valence iron oxide and it has a cubic inverse spinel structure with a unit cell axis of 8.4045(4) Å at ambient conditions (Inorganic Crystal Structure Database no. 082234). Effects of particle size on the cell parameters and lattice symmetry have been observed for several oxides,[22] and an expansion of the lattice constants is associated with a decrease in particle size for most non-metallic solids.[23] In few cases, for example, Fe_2O_3, these size effects are large enough to cause a structural transition.[24] For a large class of oxides it has been proposed that the decrease in particle size has the same effect as the application of a negative pressure on the lattice leading to an expansion in lattice cell volume.[22–25] The size effect is typically reported for a few particle sizes, however, the in situ study presented herein reports hundreds of unit cell values that can be correlated with particle sizes ranging from 5 to 25 nm providing much stronger confirmation of the phenomenon (Figure 2a–c). There is a large decrease in the unit cell parameters with increasing particle size up to a crystallite size of a about 13 nm followed by a gradual decrease until the limiting bulk value is reached at about 25 nm. The decrease possibly relates to the gradual decrease in iron(II) content and inclusion of iron(III).[25]

The heating profile of the reactant in a continuous-flow synthesis resembles the thermal profiles obtained from the pulsed injection used in the present study (see the Supporting Information). The insight gained from the present experiment therefore relates directly to the continuous-flow synthesis and the in situ data suggest that it is possible to obtain magnetite nanoparticles of around 5 nm with a narrow size distribution, that is, in the superparamagnetic state,[26] without adding surfactants. To demonstrate the application of the in situ information we have carried out the continuous-flow synthesis of gram-scale quantities of highly crystalline magnetite nanoparticles with an average size of 6 nm (Figure 4) and a specific surface area of 120 $m^2 g$. In previous continuous-flow studies in supercritical water much larger particles sizes (ca. 50 nm) were obtained.[19] For details of the synthesis conditions, see the Supporting Information.

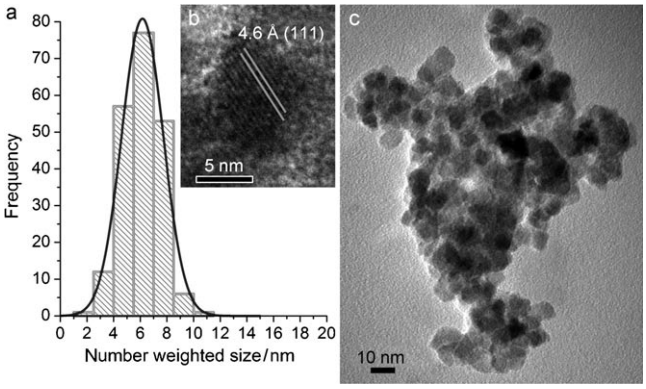

Figure 4. a) TEM size distribution of magnetite nanoparticles obtained from a gram-scale production using the continuous-flow supercritical synthesis. b) HR-TEM image of a single magnetite nanocrystal displaying (111) lattice fringes. c) A representative TEM image used for particle size statistics.

In summary, we have performed a one-step synthesis of pure phase and fully crystalline magnetite nanoparticles in an environmentally friendly medium in less than one minute. Most synthesis methods for small magnetite nanoparticles use organic stabilization to obtain size control. The fast heating rates of the present method allow very short reaction times under controlled and reproducible conditions, and thus stabilizers are not required. The study demonstrates that control over the synthesis process can be obtained based on insights of a time-resolved in situ SAXS/WAXS experiment, which has been carried out for the first time under supercritical water condition. As proof of concept, superparamagnetic magnetite nanoparticles with an average size of 6 nm and a narrow size distribution were synthesized in large-scale, offering great potential for industrial applications. The experimental methodology introduced here offers a general solution to in situ studies in supercritical water, thus providing a fundamental understanding of the interplay between the structure and properties of nanocrystalline materials.

Experimental Section

The X-ray measurements were performed at beamline 1ID at the Advanced Photon Source, Argonne National Laboratory. The reactor was developed specifically for these experiments. Pulses of $C_6H_8O_7FeNH_3$ (1.0 M, 0.7 mL, RT) was injected at 300 bar into the preheated reactor by a pulsed pneumatic pump, resulting in initial heating rates of 25–100 °C s^{-1}.

Continuous hydrothermal synthesis were performed using the flow reactor described elsewhere.[17] Preheated water and an aqueous solution of $C_6H_8O_7FeNH_3$ (0.20 M) were mixed continuously at 300 bar at flow rates of 5.0 mL min^{-1}. Further experimental details are provided in the Supporting Information.

Received: February 24, 2009
Published online: May 27, 2009

Keywords: crystal growth · magnetite · nanostructures · supercritical fluids · X-ray diffraction

[1] S. H. Sun, C. B. Murray, D. Weller, L. Folks, A. Moser, *Science* **2000**, *287*, 1989.
[2] J. Xie, K. Chen, H. Y. Lee, C. J. Xu, A. R. Hsu, S. Peng, X. Y. Chen, S. H. Sun, *J. Am. Chem. Soc.* **2008**, *130*, 7542.
[3] R. Jurgons, C. Seliger, A. Hilpert, L. Trahms, S. Odenbach, C. Alexiou, *J. Phys. Condens. Matter* **2006**, *18*, S2893.
[4] C. Alexiou, R. J. Schmid, R. Jurgons, M. Kremer, G. Wanner, C. Bergemann, E. Huenges, T. Nawroth, W. Arnold, F. G. Parak, *Eur. Biophys. J. Biophys. Lett.* **2006**, *35*, 446.
[5] T. Neuberger, B. Schopf, H. Hofmann, M. Hofmann, B. von Rechenberg, *J. Magn. Magn. Mater.* **2005**, *293*, 483.
[6] H. Zhao, J. Gagnon, U. O. Häfeli, *BioMagn. Res. Tech.* **2007**, *5*:2.
[7] J. H. Wu, S. P. Ko, H. L. Liu, S. Kim, J. S. Ju, Y. Keun-Kim, *Mater. Lett.* **2007**, *61*, 3124.
[8] Y. Deng, L. Wang, W. Yang, S. Fu, A. Elaissari, *J. Magn. Magn. Mater.* **2003**, *257*, 69.
[9] Y. Lee, J. Lee, C. J. Bae, J. G. Park, H. J. Noh, J. H. Park, T. Hyeon, *Adv. Funct. Mater.* **2005**, *15*, 503.

[10] U. T. Lam, R. Mammucari, K. Suzuki, N. R. Foster, *Ind. Eng. Chem. Res.* **2008**, *47*, 599.
[11] J. Park, K. An, Y. Hwang, J. E. G. Park, H. J. Noh, J. Y. Kim, J. H. Park, N. M. Hwang, T. Hyeon, *Nat. Mater.* **2004**, *3*, 891.
[12] M. Fernández-García, A. Martinez-Arias, J. C. Hanson, J. A. Rodriguez, *Chem. Rev.* **2004**, *104*, 4063.
[13] P. Norby, *Curr. Opin. Colloid Interface Sci.* **2006**, *11*, 118.
[14] F. Lupo, J. K. Cockcroft, P. Barnes, P. Stukas, M. Vickers, C. Norman, H. Bradshaw, *Phys. Chem. Chem. Phys.* **2004**, *6*, 1837.
[15] W. Fan, M. Ogura, G. Sankar, T. Okubo, *Chem. Mater.* **2007**, *19*, 1906.
[16] H. Jensen, M. Bremholm, R. P. Nielsen, K. D. Joensen, J. S. Pedersen, H. Birkedal, Y. S. Chen, J. Almer, E. G. Sogaard, S. B. Iversen, B. B. Iversen, *Angew. Chem.* **2007**, *119*, 1131; *Angew. Chem. Int. Ed.* **2007**, *46*, 1113.
[17] J. Becker, P. Hald, M. Bremholm, J. S. Pedersen, J. Chevallier, S. B. Iversen, B. B. Iversen, *ACS Nano* **2008**, *2*, 1058. Conventionally a slightly different weighting factor ($< D^4 > / < D^3 >$) is used. The derivation of the $(< D^8 > / < D^6 >)^{1/2}$ weighting factor will be given in a forthcoming publication (J. S. Pedersen, unpublished results). None of the conclusions presented in the paper are dependent on the explicit form of the weighting factor.
[18] T. Adschiri, Y. Hakuta, K. Arai, *Ind. Eng. Chem. Res.* **2000**, *39*, 4901.
[19] T. Adschiri, K. Kanazawa, K. Arai, *J. Am. Ceram. Soc.* **1992**, *75*, 1019.
[20] R. M. Cornell, W. Schneider, *Polyhedron* **1989**, *8*, 149.
[21] K. J. Ziegler, R. C. Doty, K. P. Johnston, B. A. Korgel, *J. Am. Chem. Soc.* **2001**, *123*, 7797.
[22] P. Ayyub, V. R. Palkar, S. Chattopadhyay, M. Multani, *Phys. Rev. B* **1995**, *51*, 6135.
[23] V. R. Palkar, P. Ayyub, S. Chattopadhyay, M. Multani, *Phys. Rev. B* **1996**, *53*, 2167.
[24] P. Ayyub, M. Multani, M. Barma, V. R. Palkar, R. Vijayaraghavan, *J. Phys. C* **1988**, *21*, 2229.
[25] D. Thapa, V. R. Palkar, M. B. Kurup, S. K. Malik, *Mater. Lett.* **2004**, *58*, 2692.
[26] A.-H. Lu, E. L. Salabas, F. Schüth, *Angew. Chem.* **2007**, *119*, 1242; *Angew. Chem. Int. Ed.* **2007**, *46*, 1222.

